

SORTING AND RETENTION OF THE GOLGI FORM OF THE V-TYPE
ATPASE IN YEAST

by

GLEN EMERSON CRONAN

A DISSERTATION

Presented to the Department of Biology
and the Graduate School of the University of Oregon
in partial fulfillment of the requirements
for the degree of
Doctor of Philosophy

June 2011

DISSERTATION APPROVAL PAGE

Student: Glen Emerson Cronan

Title: Sorting and Retention of the Golgi Form of the V-type ATPase in Yeast

This dissertation has been accepted and approved in partial fulfillment of the requirements for the Doctor of Philosophy degree in the Department of Biology by:

Bruce Bowerman	Chairperson
Tom H. Stevens	Advisor
Karen Guillemin	Member
George F. Sprague Jr.	Member
Kenneth E. Prehoda	Outside Member

and

Richard Linton	Vice President for Research and Graduate Studies/Dean of the Graduate School
----------------	--

Original approval signatures are on file with the University of Oregon Graduate School.

Degree awarded June 2011

© 2011 Glen Emerson Cronan

DISSERTATION ABSTRACT

Glen Emerson Cronan

Doctor of Philosophy

Department of Biology

June 2011

Title: Sorting and Retention of the Golgi Form of the V-type ATPase in Yeast

Approved: _____
Tom H. Stevens

Regulated acidification of intercellular organelles and vesicles is essential for many cellular processes, from basic metabolism and protein sorting to synapse function and developmental signaling. These diverse processes are driven by spatiotemporal regulation of the V-ATPase, the cellular H⁺-pump. In yeast and higher eukaryotes V-ATPase localization is directed by the 100-kDa “a” subunit, and many human diseases are linked to mutations in “a”. *Saccharomyces cerevisiae* contains two “a” isoforms, *VPH1* and *STV1*, with all other V-ATPase subunits encoded for by single genes. The V-ATPase contains only one “a” subunit per complex. Complexes that contain Vph1p localize to the vacuole (lysosome), and Stv1p-containing complexes localize to the late Golgi/endosome. Here I present a set of *STV1* mutants that are disrupted for Golgi retention but not V-ATPase assembly or enzymatic function. Using a forward genetic screen I defined multiple residues within a 39 amino-acid region of Stv1p that are necessary for Stv1p retention to the Golgi. The residues most strongly affecting Golgi localization are present in a small *STV1*-specific insertion of eight residues,

suggesting they may bind directly to sorting machinery. However, I also find that Stv1p/Vph1p chimeras containing the *STVI*-specific insertion are not sufficient to direct Golgi retention in both minimal (13AA) and expanded (49AA) contexts. I conclude that the Stv1p Golgi retention signal is composed of a complex binding surface, of which the central element is a short peptide rich in amino acids with aromatic side chains.

CURRICULUM VITAE

NAME OF AUTHOR: Glen Emerson Cronan

GRADUATE AND UNDERGRADUATE SCHOOLS ATTENDED

University of Oregon, Eugene OR
Beloit College, Beloit WI

DEGREES AWARDED:

Doctor of Philosophy, Biology, 2011, University of Oregon
Bachelor of Science, Biochemistry, 2002, Beloit College

AREAS OF SPECIAL INTEREST:

Genetics
Molecular Biology
Biochemistry

PROFESSIONAL EXPERIENCE:

Research Assistant, Dr. David Keating, Loyola University Medical Center,
2002-2004

Graduate Teaching Fellow, Department of Biology, University of Oregon,
2004-2005

Graduate Research Fellow, Institute of Molecular Biology, University of Oregon,
2005-2007, 2010-2011

GRANTS, AWARDS, AND HONORS

American Heart Association Pre-Doctoral Fellow, University of Oregon, 2007-2009

PUBLICATIONS:

Cronan GE, Keating DH, *Sinorhizobium meliloti* sulfotransferase that modifies lipopolysaccharide. *Journal of Bacteriology*, 2004 **186**(13): p4168-76

ACKNOWLEDGMENTS

I would like to thank my advisor, Tom, for supporting me through thick and thin and for providing an infectious optimism when things looked bleak. Thank you to the Stevens Lab, particularly Dr. Laurie A. Graham, whose brilliance at the bench saved my project on several occasions. To my good friends, Astra, Charles, Brit, et al., words cannot express the depths of my appreciation for all your help, both scientific and otherwise. Lastly, thank you to my father and brother for their love and support.

I would like to thank the American Heart Association for providing funding for this project.

This manuscript is dedicated to the memory of my mother, Elizabeth J. Cronan.

TABLE OF CONTENTS

Chapter	Page
I. AN INTRODUCTION TO PROTIEN SORTING AND THE V-ATPASE IN YEAST.....	1
II. IDENTIFICATION OF <i>STVI</i> MUTANTS THAT ARE DEFECTIVE FOR GOLGI-RETENTION.....	7
A Genetic Screen Identifies the Stv1p Golgi-Retention Signal.....	10
Trp ₈₃ -Lys-Tyr Is Required for Efficient Retention of Stv1p V-ATPase to the Golgi.....	21
Stv1p/Vph1p Chimeras Containing the Residues Necessary for Stv1p Golgi-Retention Fail to Localize to the Golgi.....	27
III. DISCUSSION.....	30
APPENDIX: MATERIALS AND METHODS.....	36
REFERENCES CITED.....	42

LIST OF FIGURES

Figure		Page
1.	Sorting of the yeast V-ATPase.....	9
2.	Stv1p V-ATPase Golgi localization is maintained via a saturable retention mechanism.....	12
3.	Isolation of Stv1p mutants disrupted for Golgi-retention.....	16
4.	Mutant analysis identified the <i>STV1</i> residues Phe ₅₀ and Trp ₈₃ -Lys-Tyr as necessary for retention of the Stv1p V-ATPase to the Golgi/endosomal network.....	18
5.	Mutant Stv1p V-ATPase is mislocalized to, and acidifies the vacuole. Mislocalization is not due to overexpression.....	19
6.	Single and multiple amino acids necessary for Golgi-targeting of the Stv1p V-ATPase.....	22
7.	Summary of the residue changes made in the Phe ₅₀ to Trp ₈₃ -Lys-Tyr region of Stv1p.....	23
8.	Disruption of Trp ₈₃ , Tyr ₈₅ results in mislocalization of Stv1p V-ATPase to the vacuole, and vacuolar acidification. Mislocalization is not due to overexpression of Stv1p.....	25
9.	The Trp ₈₃ -Lys-Tyr region of Stv1p is not sufficient to cause Vph1p to be retained to the Golgi.....	29

LIST OF TABLES

Page	Table	
	1.	Summary of randomly isolated mutant amino acid changes and zinc resistance..... 41

CHAPTER I
AN INTRODUCTION TO PROTIEN SORTING AND THE
V-ATPASE IN YEAST

The budding yeast *Saccharomyces cerevisiae* is one of the best studied eukaryotic model systems, and has proved to be an invaluable model for investigating the molecular mechanisms of membrane trafficking. The intracellular organelles of eukaryotic cells contain distinct lipid and protein components necessary for their form and function. Each organelle performs distinct cellular processes and the sorting of proteins to, and between, organelles is required both for organelle and protein function. Many proteins destined for organelles or secretion are transported through, or inserted into the membrane of the endoplasmic reticulum (ER) (NICCHITTA 2002). The majority of these ER-localized proteins are then packaged into ER-derived membrane vesicles for transport to the Golgi apparatus. While transiting the Golgi many proteins receive post-translational modifications before being packaged into Golgi-derived vesicles destined for either the plasma membrane or other cellular compartments such as the endosome and/or lysosome/vacuole.

The yeast vacuole, the functional equivalent of the lysosome in mammalian cells, is the most prominent cellular organelle and is easily identifiable by light microscopy. The vacuole contains a unique assortment of proteins, and also provides an acidified luminal environment of $\text{pH} \approx 5.5$ (PRESTON *et al.* 1989). The vacuole helps to regulate cellular homeostasis by affecting osmoregulation, cytosolic ion and pH homeostasis, storage of metabolites, removal of toxic substances and macromolecular degradation and

recycling (NISHI and FORGAC 2002). Vacuolar acidification is required to drive many of these processes via coupled transport.

The Golgi-endosomal membrane network is also acidified in eukaryotic cells as diverse as yeast and humans (PERRET *et al.* 2005). The acidification of the Golgi-endosomal network of membranes is important for cells to maintain efficient receptor recycling, intracellular targeting of proteins, and many other cellular processes such as protein processing and degradation (NISHI and FORGAC 2002).

The luminal pH of the Golgi/endosome/vacuole network is generated and maintained by the vacuolar-type proton-translocating ATPase (V-ATPase). The V-ATPase, is formed from two discrete multi-subunit domains; the membrane associated H⁺-translocating V_o domain, and the cytosolic ATP catalytic V₁ domain (GRAHAM and STEVENS 1999). These domains are assembled separately and can reversibly associate, dependent on cellular conditions (KANE 1995). The V_o domain is assembled in the ER and is transported to the vacuole by vesicle transport via the Golgi/endosome (HILL and STEVENS 1994; KAWASAKI-NISHI *et al.* 2001; MALKUS *et al.* 2004). The V₁ domain is assembled in the cytosol, and assembles with the V_o domain within minutes (PARRA and KANE 1998).

The V-ATPase is one of the smallest know molecular motors that functions by a rotational mechanism. The mechanism is analogous to that of the F₁F₀ class of ATPases, but is reversed with respect to proton flow/ATP catalysis. i.e. The V-ATPase captures energy from the hydrolysis of ATP and uses it to drive protons across the organelle membrane, creating an electro-chemical gradient. The V₁ subdomain is comprised of

eight subunits termed A-H, and the V_0 subdomain is composed of six subunits designated a, d, c, c', c'', and e. The V_1 is hydrophilic and resides in the cytoplasm, the V_0 is hydrophobic and spans the lipid bilayer of the resident organelle. Subunits A and B of V_1 contain the ATP binding and catalytic domains and form a ring-like structure from three A-B dimers. Subunits c, c', and c'' of V_0 also form a ring structure, most likely composed of four copies of c and one copy each of c' and c'' (WANG *et al.* 2007). The V_1 and V_0 rings are rotationally coupled by V_0 subunits D and F and these two rings rotate with respect to the stator subunit, designated “a”. The interface between the V_0 ring and “a” constitutes a “proton pore”, a channel through which protons flow, as a result of V_1/V_0 rotation with respect to “a”. The remaining subunits either play regulatory roles (C and H) or act as a “peripheral stator” (E and G) (TOEI *et al.* 2010).

The V-ATPase shares structural homology to the F_1F_0 class of ATPases and is found in the membranes of all acidified organelles such as the Golgi, endosomes, vacuoles, and lysosomes (NISHI and FORGAC 2002). In higher order eukaryotes the V-ATPase is dynamically recruited to distinct vesicle populations where it is required for complex processes such as neurotransmitter release (DI GIOVANNI *et al.*), and Wnt signal transmission (CRUCIAT *et al.*). However these higher order eukaryotes present significant experimental difficulties as many of the 14 subunits of the V-ATPase are encoded by multiple genes (SUN-WADA *et al.* 2003), whereas in yeast 13 of the 14 subunits are encoded by single genes. The only V-ATPase subunit encoded by two genes in yeast is the 100 kD V_0 “a” subunit. The V-ATPase “a” subunit has 4 isoforms in mammals, and each of the four genes is expressed in a tissue-specific manner and their mRNAs are

differentially spliced (NISHI and FORGAC 2000; OKA *et al.* 2001). Multiple “a” isoform-specific phenotypes have been recently discovered: V-ATPase “a” subunit “a3” isoform has been shown to regulate insulin secretion from pancreatic beta-cells in mouse (SUNWADA *et al.* 2006), and in humans mutations in the “a3” and “a4” isoforms can result in osteoporosis (KORNAK *et al.* 2000; SOBACCHI *et al.* 2001) and distal renal tubular acidosis (SMITH *et al.* 2000). The V-ATPase has been shown to regulate pH and cell migration in microvascular endothelial cells, a cell type critical for angiogenesis (ROJAS *et al.* 2006). Additionally, RNAi knockdowns of isoforms of “a3” and “a4” have been shown to diminish the invasiveness of human tumor cells, indicating that V-ATPase localization may act as a positive effector of tumor cell metastasis (HINTON *et al.* 2009).

Although yeast is a simple eukaryote, the V-ATPase complexes localize to different compartments depending on which V_o “a” subunit is present in the complex (MANOLSON *et al.* 1994). This differential localization is of great interest because understanding this localization is critical to understanding the physiological functions of the various human V-ATPase isoforms (OCHOTNY *et al.* 2006). Although loss of function mutations affecting the V-ATPase are embryonic lethal in animals, yeast V-ATPase null mutants (Vma⁻) are conditionally viable. Deletion of any of the yeast V-ATPase subunit genes, or both “a” subunits, results in identical phenotypes: failure to acidify the vacuole, sensitivity to elevated extracellular concentrations of Ca²⁺ and Zn²⁺, and failure to grow above pH 7 (MANOLSON *et al.* 1994; NELSON and NELSON 1990). The two yeast “a” subunit isoforms are encoded by *VPH1* and *STV1*, and both of these genes must be deleted to give a Vma⁻ phenotype (MANOLSON *et al.* 1994). The Stv1 and

Vph1 proteins exhibit 54% amino acid identity, and whereas the Vph1p-containing V-ATPase localizes to the vacuole membrane (MANOLSON *et al.* 1992), the Stv1p-containing V-ATPase localizes to Golgi and endosomal membranes (MANOLSON *et al.* 1994) (Figure 1). Characterization of the mechanism by which the Stv1p V-ATPase is retained in the Golgi revealed continual recycling by retrieval from the endosome back to the Golgi (KAWASAKI-NISHI *et al.* 2001).

Continual cycling of membrane proteins between the Golgi and endosomes has been demonstrated for a number of other yeast proteins, and in some cases a short peptide sequence within these proteins has been identified that is required for recycling. Ste13p is retained in the Golgi by one such peptide signal sequence: FXFXD (BRYANT and STEVENS 1997; NOTHWEHR *et al.* 1993). Although this peptide sequence is present in Stv1p, deletion of this motif did not alter the localization of the Stv1p V-ATPase (KAWASAKI-NISHI *et al.* 2001), suggesting that a novel retention signal may be present in Stv1p. Studies using Stv1p-Vph1p chimeras demonstrated that the region of Stv1p required for Golgi localization resides in the N-terminal half of the protein (KAWASAKI-NISHI *et al.* 2001). Interestingly, these chimeras exhibited enzymatic properties dependent on the “a” subunit C-terminal domain but localization dependent on the N-terminal domain (LENG *et al.* 1998). A number of additional Stv1p-Vph1p chimeras and in-frame deletions were constructed in an effort to define more precisely the N-terminal region of Stv1p required for Golgi localization. However, only one of the resulting mutants (a deletion removing the FXFXD motif) resulted in a Stv1p V-ATPase capable of exiting the endoplasmic reticulum (ER), demonstrating that correct folding of

the Stv1p N-terminal domain is required for correct V-ATPase assembly and ER exit (KAWASAKI-NISHI *et al.* 2001).

Further insights into the sorting mechanism for the Stv1p-containing V-ATPase have come from experiments in yeast that overexpress Stv1p; these cells show accumulation of Stv1p V-ATPase on the vacuole (MANOLSON *et al.* 1994). Although the vacuoles of yeast cells deleted for *VPH1* (*vph1Δ*) do not become acidified, *vph1Δ* cells overexpressing Stv1p have acidified vacuoles due to the vacuolar localization of missorted Stv1p-containing V-ATPase complexes (MANOLSON *et al.* 1994) (Figure 2). This supports the hypothesis that sorting of the Stv1p V-ATPase is an active process, and that this Stv1p V-ATPase complex is retained by a saturable endosome to Golgi retrieval mechanism, as is seen for other yeast Golgi membrane proteins (ROBERTS *et al.* 1992; WILCOX *et al.* 1992).

In this work we identify mutants of Stv1p that are disrupted for Golgi retention but still retain wild-type levels of assembly and enzymatic function. Furthermore, we leverage information about the location of these necessary residues to design and test two STV1/VPH1 genetic chimeras containing one or both regions of Stv1p found to be necessary for the retention of Stv1p V-ATPase to the Golgi. These chimeras, while fully functional, were not retained to the Golgi suggesting that the Stv1p Golgi retention signal is comprised of a complex binding surface.

CHAPTER II

IDENTIFICATION OF *STV1* MUTANTS THAT ARE DEFECTIVE FOR GOLGI-RETENTION

Saccharomyces cerevisiae contains two isoforms of the 100 kilodalton “a” subunit, Stv1p and Vph1p. A single “a” subunit is present per complex, and V-ATPase containing Vph1p or Stv1p localize to the vacuole (lysosome in mammals) and Golgi respectively. This lab previously demonstrated that the Golgi targeting information resides within the N-terminal 455 residues of Stv1p (KAWASAKI-NISHI *et al.* 2001). This initial finding was realized by immunolocalization of a functional Stv1p/Vph1p genetic chimera that approximately bisected the proteins, swapping the hydrophilic and hydrophobic domains of the two “a” isoforms. Design of this chimera was based on both primary amino acid sequence homology and secondary structure predictions, as no high resolution structural data existed, or indeed currently exists, for either “a”. However, despite the success of this experiment, dozens of attempts to more precisely define the Stv1p Golgi retention signal using genetic chimeras have been unsuccessful (data not shown). The reason for the frequent failure of these chimeric approaches lies in the complexity of V-ATPase assembly. At least five non-subunit proteins participate in V_0 assembly and of those five, three are absolutely essential to the V-ATPase assembly process (DAVIS-KAPLAN *et al.* 2006; GRAHAM and STEVENS 1999; RYAN *et al.* 2008). These assembly factors reside in the ER and function as a “checkpoint” for correct V-ATPase assembly. Only V_0 deemed to be correctly assembled is allowed to proceed out of the ER to transit the biosynthetic pathway. V_0 deemed to be incorrectly assembled

fails to exit the ER and the “a” subunit is rapidly degraded. Many additional chimeras made by myself and others failed this stringent quality control check. As no post-ER localization information can be obtained for these assembly-deficient alleles of “a”, these chimeras were ultimately uninformative as to the nature of the *STVI* Golgi retention signal. Given the difficulties inherent to chimeric approaches I sought to define amino acids necessary for correct function of the Stv1p Golgi-targeting signal using a forward genetic screen. Here I describe a set of *STVI* mutant alleles disrupted for Golgi retention but that still retain wild-type levels of assembly and enzymatic function. I then used this information to create precisely targeted Stv1p/Vph1p chimeras that contain the region of Stv1p already defined as necessary. These minimal Stv1p/Vph1p chimeras exhibited wild-type levels of assembly and enzymatic function but were not retained to the Golgi.

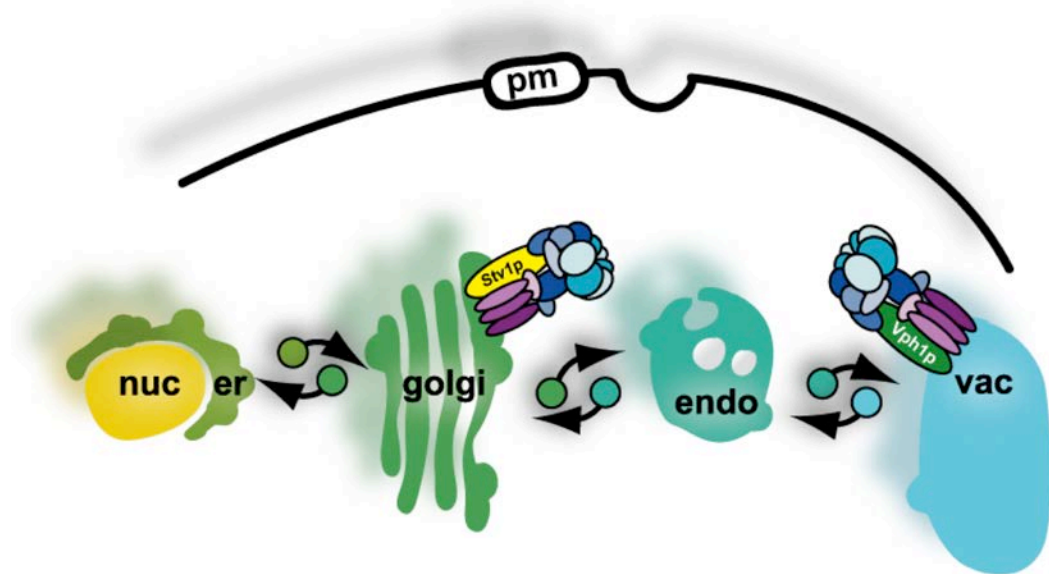


Figure 1. Sorting of the yeast V-ATPase

V-ATPase complexes containing the “a” subunit Stv1p localize to the Golgi by cycling/recycling from the endosome. V-ATPase complexes containing “a” subunit Vph1p localize to the vacuole.

A Genetic Screen Identifies the Stv1p Golgi-Retention Signal

In order to define the Stv1p Golgi-retention signal by forward genetics I required a cellular-level growth phenotype that was sensitive to V-ATPase location. Calcium resistance, the most widely used assay for V-ATPase function, is not dependent on V-ATPase location; cells can acidify either their Golgi or vacuole and still be resistant to calcium. In stark contrast to calcium resistance, zinc-resistance has been shown to specifically require vacuolar acidification (MANOLSON *et al.* 1994). I reasoned that this peculiarity of zinc resistance could be leveraged in a genetic screen to couple intercellular V-ATPase localization and growth; allowing me to select for mutant alleles of *STV1* that were disrupted for Stv1p Golgi retention. Importantly, any identified mutants must retain near WT levels of V-ATPase activity in order to be zinc resistant, a condition that precludes their having significant defects in V-ATPase assembly or enzymatic function.

Stv1p V-ATPase resides at steady state within the Golgi complex. Overexpression of Stv1p in cells lacking the vacuolar isoform (*vph1Δ*) causes mislocalization of a population of Stv1p V-ATPase to the vacuole, presumably by saturation of the Golgi retention machinery (MANOLSON *et al.* 1994). I confirmed that overexpression of Stv1p caused its mislocalization to the vacuole by expressing an HA-tagged allele of *STV1* from a high copy plasmid in *vph1Δ* cells and visualizing Stv1p localization by indirect immunofluorescence (Figure 2a). To confirm that vacuolar-localized Stv1p V-ATPase is functional I assayed the same strain for cellular zinc resistance and observed a large increase in growth compared to the WT control (Figure

2b). Finally, I directly assayed Stv1p-dependent vacuolar acidification using the fluorescent dye quinacrine. Quinacrine can freely traverse membranes in its unprotonated form but becomes trapped in acidified compartments in its protonated form, causing them to fluoresce. Quinacrine staining provides direct evidence that vacuolar-localized Stv1p V-ATPase is enzymatically functional (Figure 2c).

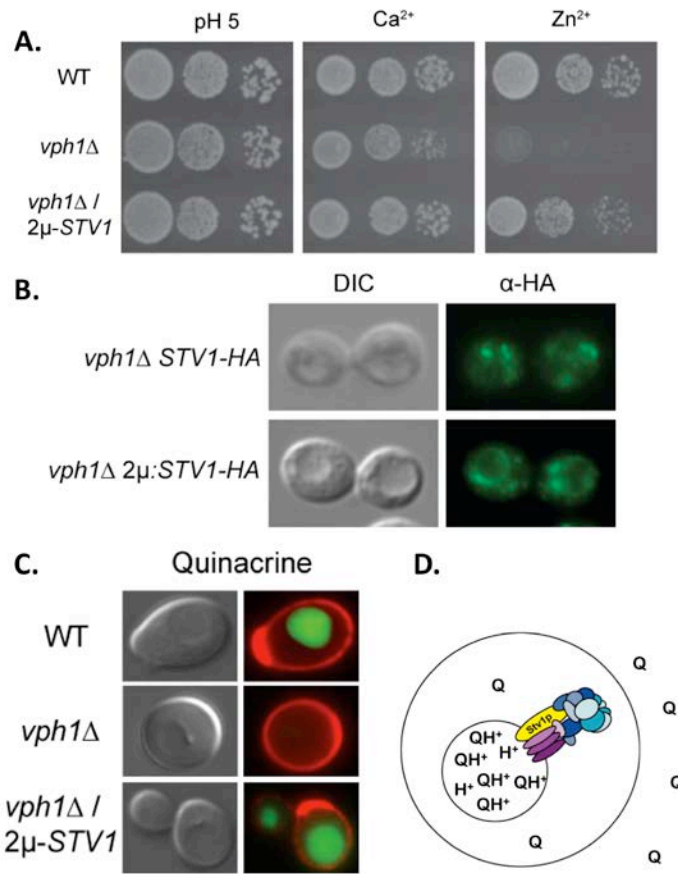


Figure 2. *Stv1p* V-ATPase Golgi localization is maintained via a saturable retention mechanism

A. Wild-type (WT) and *vph1*Δ were transformed with either a high-copy control plasmid (YEp352) or the same plasmid expressing *Stv1p* from its endogenous promoter (2μ-*STV1*). Strains were grown to exponential phase, serially diluted and spotted on YEPD pH5 (pH5) and YEPD (unbuffered) + 1 mM ZnCl₂ (Zn²⁺). **B.** Indirect immunofluorescence microscopy of *vph1*Δ cells expressing a HA-tagged allele of *STV1* from either the genomic locus (*STV1*-HA), or from a high-copy (2μ-*STV1*-HA) plasmid. The left panels show differential contrast microscopy (DIC) images and the right panels *Stv1p* as visualized by a fluorophore conjugated antibody stack directed against the HA epitope. **C.** The same strains as in A. stained with quinacrine and concanavalin A-TRITC (detailed in materials and methods). The left panels are differential interference microscopy (DIC) images and the right panels show overlaid images of quinacrine in green and concanavalin A-TRITC in red.

Having confirmed that the mislocalization of Stv1p V-ATPase to the vacuole conferred zinc resistance, I reasoned that a targeted mutagenesis of the N-terminal region of Stv1p would yield mutant alleles of *STVI* which failed to be retained to the Golgi. As vacuolar-localized V-ATPase is sufficient to cause a significant increase in cellular zinc resistance, rare mutants that mislocalize Stv1p V-ATPase to the vacuole could be selected for on solid media containing zinc chloride. Furthermore, because growth on Zinc-containing media requires a functional V-ATPase, mutations in Stv1p that compromised V-ATPase assembly or function would not be isolated. I considered using a GFP-tagged allele of *STVI* for our screen, but live cell imaging of Stv1p-GFP displays a small amount of vacuole localization in a *vhp1Δ* background. A similar distribution is not seen by immunofluorescence imaging of an HA-tagged version of *STVI*. I suspect that the GFP-tagged allele of *STVI* is slightly compromised for Golgi retention. Additionally, Stv1p-GFP is not fully functional when assayed for calcium resistance. As my screen would be most effective when the initial vacuolar fraction of Stv1p is small in comparison to the Golgi-retained fraction we chose the HA-tagged allele for our screen. I initially attempted to integrate randomly mutagenized *STVI* directly into the genome. Unfortunately, in my hands the efficiency of genomic integration was too low to generate a sufficiently large library of primary mutants. Settling for a slightly reduced dynamic range of cellular zinc resistance I chose to express the *STVI* mutants from a low-copy, centromere-based plasmid.

Full details of the library construction are in the appendix. Briefly, I randomly mutagenized the region of the *STVI* gene corresponding to the N-terminal 455 amino

acids by mutagenic PCR, with a mutagenesis frequency of approximately 4 nucleotide changes per 1000. These randomly mutagenized fragments were co-transformed with a linearized low-copy vector containing the remainder of the *STVI* coding sequence and native promoter/terminator. The plasmid was re-circularized by host-mediated recombination between the mutagenized fragment of *STVI* and the linearized vector. Yeast cells that received and recombined both DNA fragments were able to grow on media lacking uracil. The strain background for the recombination was *vph1Δ stv1Δ* making the mutant *STVI* the only cellular source of “a” subunit. That is, only cells that correctly accomplished the recombination would be able to grow on media containing elevated levels of zinc. Primary Ura⁺ transformants were then replica-plated onto media containing 5mM ZnCl and the most zinc-resistant isolates were selected for further screening. In order to avoid selection for increases in plasmid copy number I isolated zinc resistant mutants from the original -URA plate used for replica printing.

An improbably large number of zinc-resistant mutants (842) were obtained from the primary screen, necessitating the use of a secondary screen (Figure 3a). Positive mutants were isolated from the original -URA plates, re-isolated as single colonies and used to inoculate liquid cultures in 96-well format. Mutant sets were then combined using robotics and replica printed in 1536-spot arrays onto both permissive and zinc-containing media. Each mutant was represented at sixteen-fold degeneracy, and their growth scored relative to control strains present in each array. The secondary screen reduced the number of putative mutants by ~20-fold to a total of 42. I then attempted to test individual mutants for zinc resistance by serial dilution, but discovered small

variations between individual colony sizes. I suspect that these colony size variations were due to plasmid copy number fluctuations, and that these fluctuations were responsible for the unusually large size of the primary mutant population. To eliminate any false positives due to variation of *Stv1p* expression I integrated each of the remaining 42 mutants at the genomic *STVI* locus using a “loop-in” integration technique (Figure 3b) and re-screened the new library for zinc-resistance.

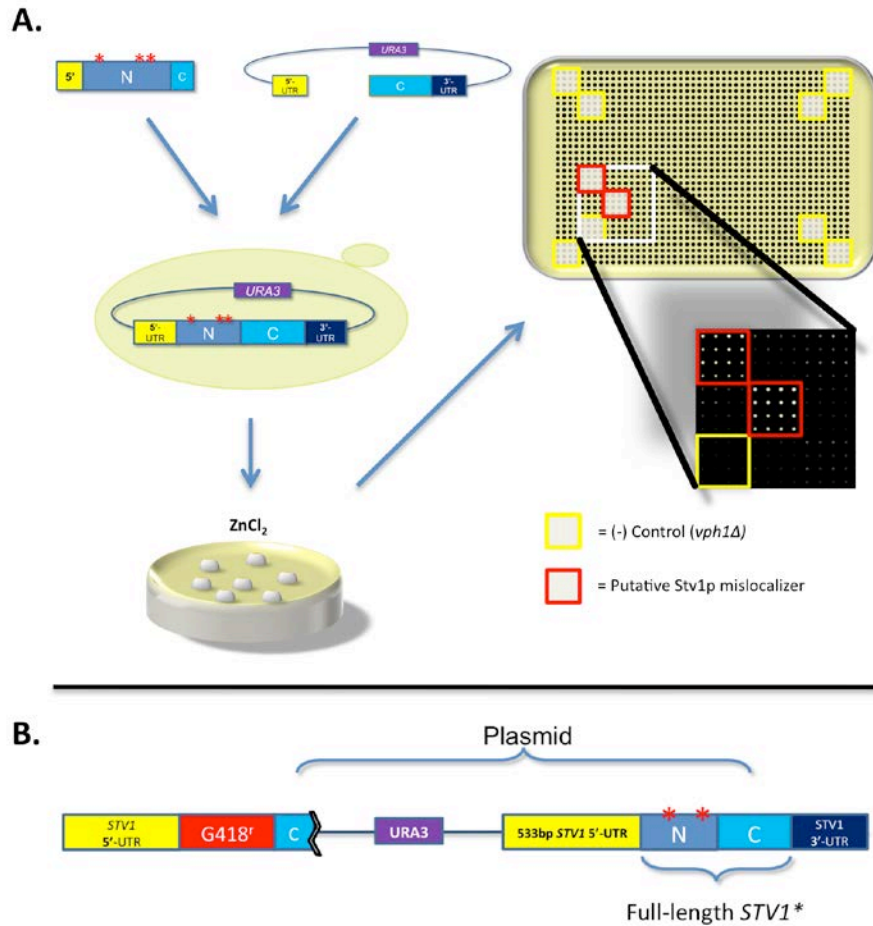


Figure 3. Isolation of *Stv1p* mutants disrupted for Golgi-retention

A. A fragment of *STV1* was randomly mutagenized by PCR and co-transformed with gapped plasmid. The fragments were re-circularized by homologous recombination in *vph1Δ stv1Δ* yeast and plasmid-containing colonies were screened by replica plating and robotic arrays on media containing zinc. Zinc resistance is indicative of vacuolar-localized *Stv1p* V-ATPase. B. Following the screens depicted in part A, mutants were integrated into *vph1Δ stv1-NTΔ* cells, restoring the *STV1* genomic locus and stabilizing *Stv1p* expression levels.

Following integration (the tertiary screen) 24 mutants displayed elevated zinc resistance when compared to controls and of those 24, 13 were scored as having a medium to strong zinc resistance phenotype. Further characterization was performed on this most phenotypically strong subset of 13 mutants. Examples and a summary of the growth data is shown in Figure 4. To determine if the mutants contained bona fide disruptions to their Golgi-retention signals I performed the experiments shown in Figure 5. First, I wished to know if the increased zinc resistance of the mutants was due to the mislocalization of the Stv1p V-ATPase to the vacuole. The integrated Stv1p mutants contained a triple hemagglutinin (HA) tag inserted after amino acid Leu₂₂₇, an allele of Stv1p shown to be Golgi-localized and fully functional by this lab (KAWASAKI-NISHI *et al.* 2001), a finding that we reconfirmed (data not shown). Using anti-HA antibodies I visualized Stv1p by indirect immunofluorescence and observed staining of the vacuolar limiting membrane in mutant, but not control cells. I then used quinacrine staining to demonstrate an increased vacuolar acidification in the mutants. Lastly, as increased expression of Stv1p can lead to its mislocalization, I assayed mutant levels of Stv1p by Western blot and observed no difference between Stv1p expression levels and the non-mutant control. These data show that the Golgi retention signal of Stv1p is disrupted in the randomly isolated mutants, and upon disruption of this signal the Stv1p-containing V-ATPase is mislocalized to and acidifies the vacuole.

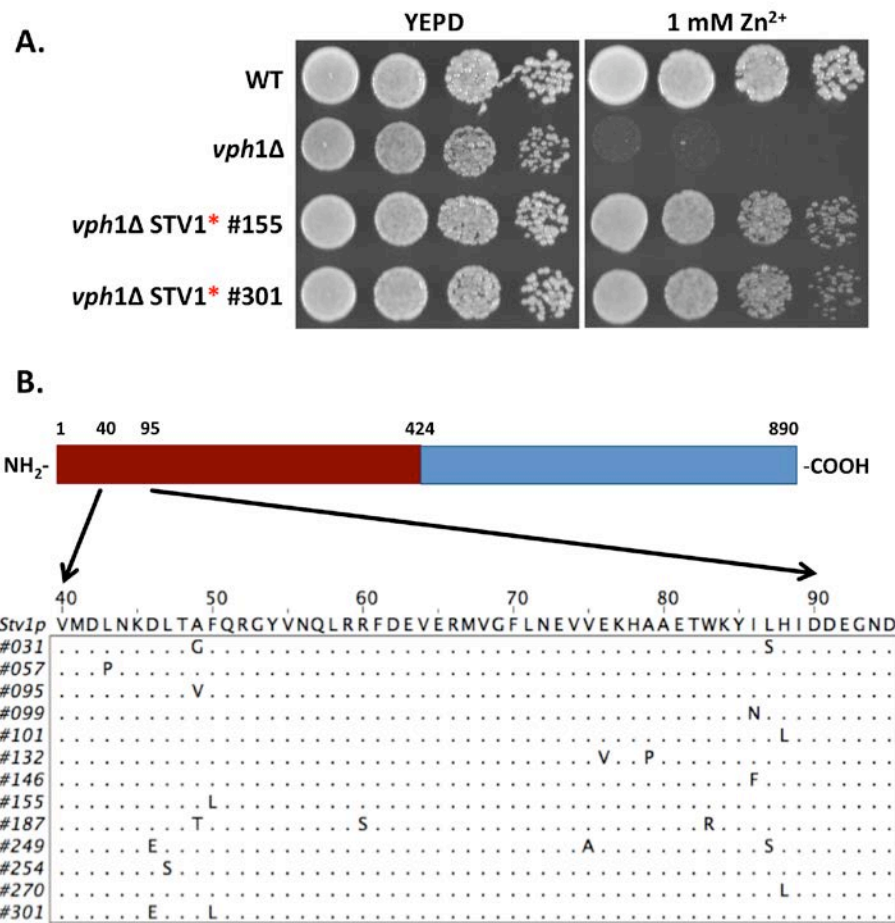


Figure 4. Mutant analysis identified the *STVI* residues (50) Phe and (83) Trp-Lys-Tyr as necessary for retention of the Stv1p V-ATPase to the Golgi/endosomal network

A. Wild-type (WT), and *vph1Δ* containing either integrated wild-type *STVI* (*vph1Δ*) or integrated mutant *STVI* (*STVI**, and mutant designation) were serially diluted (5-fold dilutions) and spotted onto permissive media (YEPD) or YEPD containing 1 mM ZnCl₂. **B.** Schematic depicting randomly isolated mutations. The red-shaded area indicates the region of Stv1p subjected to random mutagenesis. Below, the expanded region from amino acid 40 to 95 highlights amino acid change(s) found in individual zinc-resistant mutants.

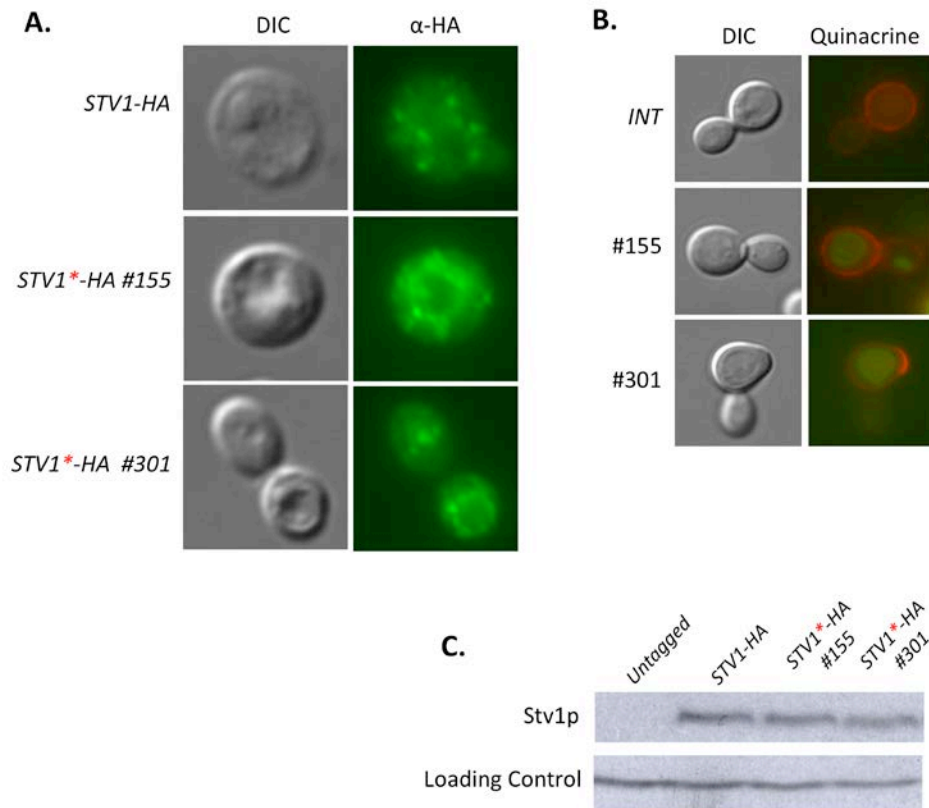


Figure 5. Mutant Stv1p V-ATPase is mislocalized to, and acidifies the vacuole. Mislocalization is not due to overexpression

A. *vph1Δ* cells containing either unmutagenized *STV1* (*STV1-HA*) or mutant *STV1* (*STV1*-HA* and mutant designation) that contain three copies of a hemagglutinin epitope tag (HA) were visualized by indirect immunofluorescence (α -HA) as described in the appendix, and Normarski optics (DIC). The vacuole is identifiable in the DIC image as a large indentation. **B.** DIC images (left) and overlaid fluorescent images (right) of the same strains in part A, quinacrine staining is shown as green (Quinacrine accumulates in acidified compartments), and the red staining is conA-TRITC which stains the cell wall. **C.** Western blot of the same strains from Part A. Top panel shows steady-state protein levels of Stv1p-HA in 60 μ g of whole-cell extract using α -HA antibodies and the bottom panel shows protein levels of Dpm1p, used as a loading control.

I sequenced the *STVI* coding sequence and promoter for all 42 mutants from the secondary screen at 3x coverage using traditional high-fidelity sequencing. The sequencing was completed before the results of the tertiary (integration) screen were known. As only 13 of these 42 were ultimately confirmed as Stv1-mislocalizers I used the full sequence dataset to eliminate mutations common to both the mutant and non-mutant sets. The full list of amino acid changes and zinc resistances for individual mutants is shown in Table 1 (see the Appendix for this table). I also noted that nucleotide changes of ~5/kb were found in the mutant and non-mutant pool and appeared to be evenly spread throughout the targeted (bp 1-1266) region of *STVI* (data not shown).

Interestingly, while many mutants contained multiple amino acid substitutions, upon comparison of mutant sequences by multiple sequence alignment I found that residue changes were clustered in two small regions (Figure 4b). The first, Trp₈₃-Lys-Tyr lies in a 13 AA region unique to Stv1p. The second, Phe₅₀ is conserved between Stv1p and Vph1p. I tested the necessity of these amino acids for Stv1p Golgi-retention by changing individual residues in and around these regions to alanine. Starting with the genomic integration vector containing the wild-type *STVI* sequence, I introduced nucleotide changes using site-directed mutagenesis. Introduced nucleotide changes were confirmed by sequencing of a ~600bp region surrounding the introduced mutation(s). These new *STVI* mutations were then integrated at the native *STVI* locus using the same integration method used for the randomly isolated mutants.

Trp₈₃-Lys-Tyr Is Required for Efficient Retention of Stv1p V-ATPase to the Golgi.

One region of Stv1p, Trp₈₃-Lys-Tyr (W₈₃KY), contained residues that when mutated singly or in combination produced a comparatively large increase in zinc-resistance; increases that equaled or exceeded the phenotype of the randomly isolated mutants (Figure 6a, and data not shown). This observation was intriguing because residues 83 to 91 comprise a Stv1p-specific insertion not present in Vph1p (Figure 6b), and as such may comprise an interaction surface between the V-ATPase and Golgi retention machinery. The residues that when mutated individually produced the largest increase in cellular zinc resistance were the aromatic residues Trp₈₃ and Tyr₈₅ (Figure 6a). This result also peaked my curiosity as aromatic residues are often found to directly mediate protein-protein interactions between sorting factors and cargo. In order to more thoroughly characterize this region I performed an alanine scan of residues 81 to 91. Results of the alanine scan show that residues flanking W₈₃KY have a comparatively small effect on zinc-resistance and that residues Trp₈₃ and Tyr₈₅ are the most critical for Stv1p Golgi-retention (Figure 7).

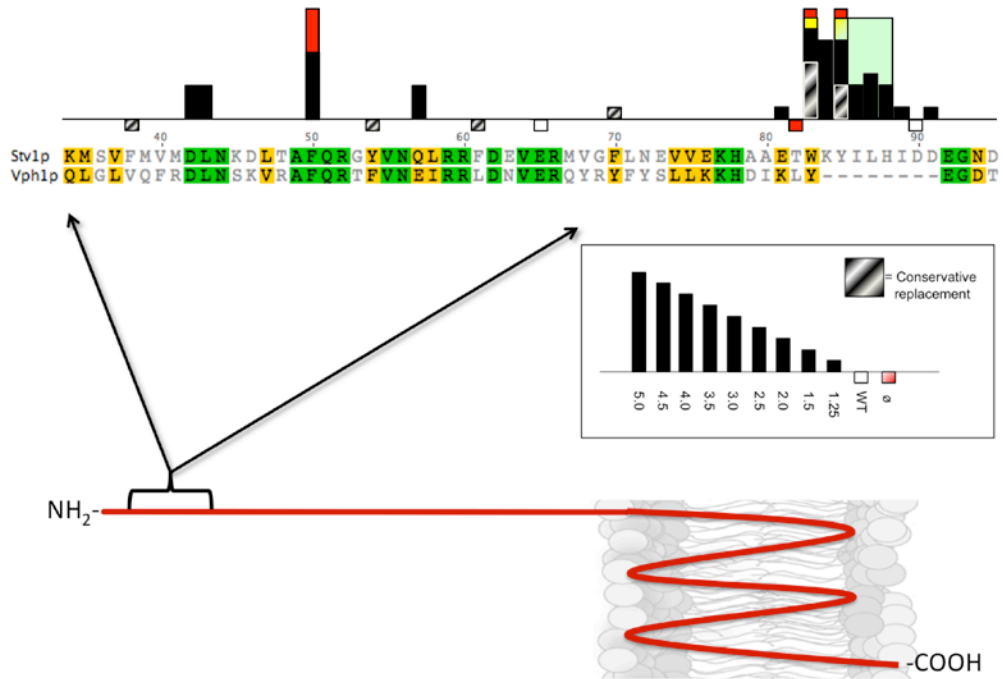


Figure 7. Summary of the residue changes made in the Phe₅₀ to Trp₈₃-Lys-Tyr region of Stv1p

Expanded view of Stv1p with the alignment to Vph1p shown in Figure 6. Bars above and below the horizontal line show the relative zinc-resistance compared to Wild Type in arbitrary units (5.0 corresponds to the zinc-resistant mutant). Conservative replacements at Stv1p positions 83 and 85 are discussed in the text, conservative changes elsewhere indicate that the Stv1p residue was changed to the corresponding Vph1p residue. Colors indicate combinatorial mutants (except for red bars that lie below the horizontal line).

In order to confirm that mutations in Trp₈₃-Lys-Tyr result in mislocalization of Stv1p V-ATPase to the vacuole, without increasing steady-state levels of Stv1p, I performed the experiments discussed below. Cells expressing mutant Stv1p with the residues changes Trp₈₃ -> Ala₈₃ and Tyr₈₅ -> Ala₈₅, present either singly (W83A and Y85A) or in combination (83AKA), display a vacuolar staining pattern by indirect immunofluorescence, while the unmutagenized control cells do not (Figure 8a - left panels, and Data not shown). Furthermore, vacuoles in the mutant cells accumulate quinacrine, demonstrating that their vacuoles are acidified (Figure 8A – right panels and Data not shown). Finally, the vacuolar localization of Stv1p in mutant cells is not due to overexpression of the mutant Stv1p as demonstrated by semi-quantitative Western blot (Figure 8b). Taken together these data indicate that replacement of the aromatic residues at positions 83 and 85 of Stv1p with alanine disrupt the Golgi-retention signal causing the mutant Stv1p V-ATPase to localize to and acidify the vacuole. More biochemically conservative substitutions were also made at positions 83 and 85: Trp₈₃ was changed to both phenylalanine and tyrosine and Tyr₈₅ was changed to phenylalanine in order to retain hydrophobic/aromatic character similar to that found in the wild-type residues. These conservative replacements caused a significant increase in zinc resistance, although the phenotypes were not as strong as those seen for the alanine changes (Figure 7).

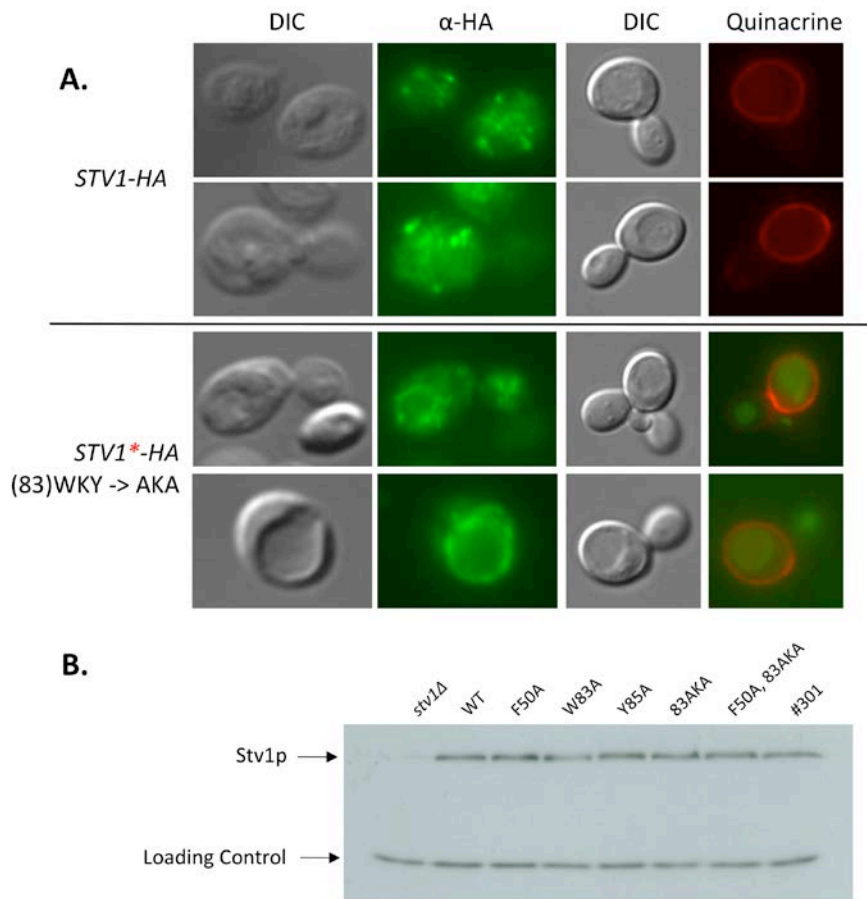


Figure 8. Disruption of Trp₈₃, Tyr₈₅ results in mislocalization of Stv1p V-ATPase to the vacuole, and vacuolar acidification. Mislocalization is not due to overexpression of Stv1p

A. DIC and indirect immunofluorescence staining of *vph1Δ* cells containing integrated wild-type *STV1* (*STV1-HA*) or *STV1* with residues Trp₈₃ and Tyr₈₅ changed to alanine (left panels). Quinacrine staining and DIC images of the same strains (right panels). **B.** Western blot of the indicated strains using α -HA antibody (Stv1p) and α -Dpm1 (Loading Control). The faint band seen in the *stv1Δ* lane is due to cross-contamination from the WT lane.

Analysis of the mutant sequence data also indicated that mutations at position Phe₅₀ of Stv1p disrupt the Golgi-retention signal (Figure 4b). In order to test this prediction I used site-directed mutagenesis to change Phe₅₀ to alanine (F50A) and found that this mutant displayed a moderately strong zinc-resistance phenotype (Figure 6a). Secondary structure predictions indicate that an alpha-helical region may lie between residues 50 and 83 of Stv1p. If so, the F50A mutation may alter the conformation of this helix and cause Stv1p mislocalization by an indirect disruption of the 83WKY motif. One prediction of this hypothesis is that 83AKA should be epistatic to F50A with respect to zinc resistance. In order to test this I combined the two mutants, making the double mutant: F50A, 83AKA. If the F50A phenotype is due solely to an indirect disruption of 83WKY (making it 83AKA-like) I would expect the zinc resistance of the double mutant (F50A, 83AKA) to equal that of 83AKA, however the double mutant was more zinc resistant than either of the single mutants (Figure 6a). This finding is remarkable, and indicates that the Stv1p Golgi-retention signal is not comprised of just a canonical sorting motif. As outlined above, discrete sorting signals are often able to direct the Golgi retention of other proteins. These signals are modular, in that they can be appended to proteins that normally localize to terminal sorting destinations (i.e. secretion) and cause the Golgi retention of the chimeric protein. Such modularity indicates that these sorting motifs fold correctly and are identified and acted upon by their cognate sorting machinery. My finding that regions of Stv1p located 40 amino acids apart independently act to direct the Golgi localization of Stv1p indicates that the V-ATPase interface with the Golgi retention machinery is more complex than was first assumed.

Stv1p/Vph1p Chimeras Containing the Residues Necessary for Stv1p Golgi-Retention Fail to Localize to the Golgi

The residues I defined as necessary for retention of the Stv1p V-ATPase to the Golgi lie between amino acids Phe₅₀ and His₈₈. As shown in Figure 6b, Phe₅₀ is conserved between Stv1p and Vph1p and as such is unlikely to bind directly to Golgi-retention factor(s). The Phe₅₀ to His₇₈ region is fairly well conserved between the “a” isoforms suggesting that these regions may form similar secondary structures in Stv1p and Vph1p. As residues 83 to 91 of Stv1p exist in a Stv1p-specific insertion I reasoned that moving these residues from Stv1p to the same context in Vph1p would cause Golgi-retention of the chimeric protein. The chimeric protein was integrated at the *STVI* locus under control of the *STVI* promoter, and is expressed at similar levels to native Stv1p (data not shown). To design this chimera I used the sequence alignment of Stv1p and Vph1p in order to identify conserved regions flanking the Stv1p-specific insertion (Figure 9b). Using this information and secondary structure predictions I chose to replace the five amino acids, 80 to 84 of Vph1p with amino acids 83 to 91 of Stv1p (Figure 9c). This 13 amino acid Stv1p-Vph1p chimera is hereafter referred to as “L1/R1”.

The L1/R1 Stv1p-Vph1p chimera displays full enzymatic function when assayed by cellular resistance to calcium (Figure 9a). If L1/R1 is retained to the Golgi less V-ATPase would be present on the vacuole causing a decrease in cellular zinc resistance.

However, L1/R1 displays identical zinc resistance compared to controls (Figure 9a), and by immunolocalization L1/R1 appears to be exclusively on the vacuole (Figure 9b).

I also constructed a *STVI/VPHI* genetic chimera containing the entire Phe₅₀ to His₇₈ region. This chimera contained 49 amino acids from Stv1p in place of 41 amino acids of Vph1p and is detailed in Figure 9c. This chimeric construct, designated “L2/R1”, was fully functional but also failed to localize to the Golgi when measured by the same assays as used for L1/R1 (Figure 9a and b).

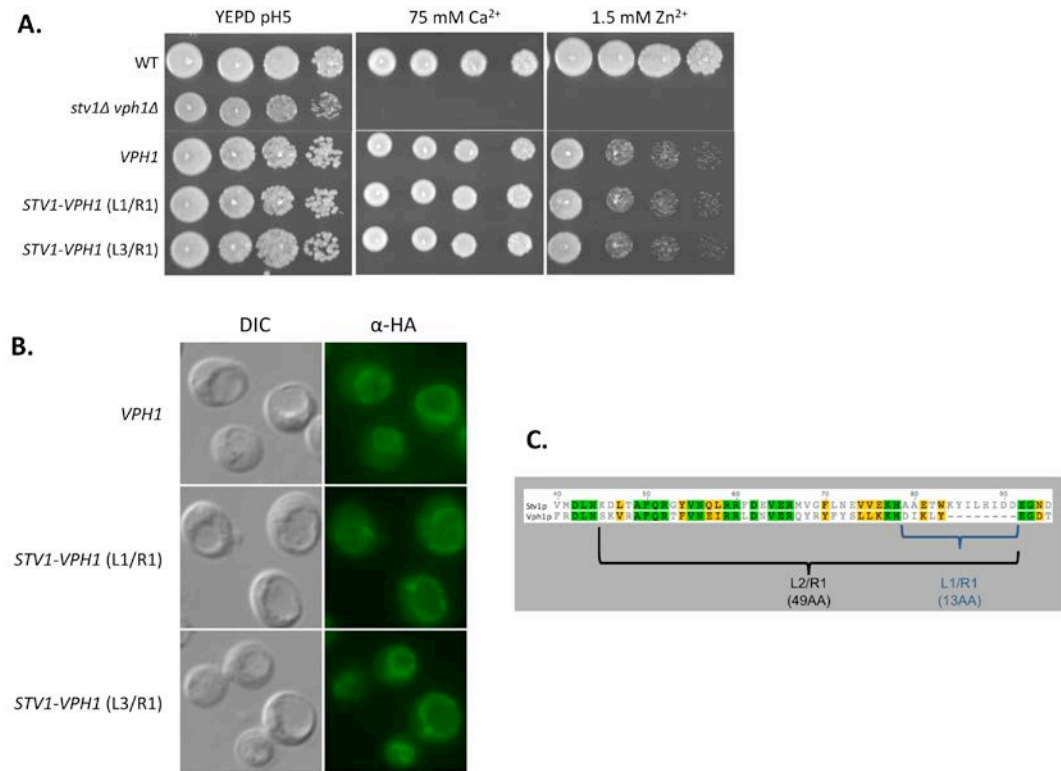


Figure 9. The Trp₈₃-Lys-Tyr region of Stv1p is not sufficient to cause Vph1p to be retained to the Golgi

A. 5-fold serial dilutions of wild-type (WT) *stv1Δ vph1Δ*, *VPH1* integrated at the *STV1* genomic locus (with *STV1* promoter), and the *STV1-VPH1* chimeras L1/R1 and L2/R1 integrated at the *STV1* genomic locus. **B.** The same strains as in Part A assayed by indirect immunofluorescence using α-HA antibody (*VPH1* and both chimeras have a 3xHA tag at their C-terminus) and DIC imaging. **C.** Schematic showing the regions of *STV1* moved to *VPH1*, and the residues of *VPH1* that were removed to create the L1/R1 and L2/R1 *STV1-VPH1* genetic chimeras.

CHAPTER III

DISCUSSION

This project aimed to more thoroughly characterize the signal in Stv1p that causes retention of the Stv1p V-ATPase to the late Golgi compartment. Previous work indicated that Stv1p is maintained at steady-state in the Golgi, at least in part, by retrograde transport from the endosome to the Golgi. This retrograde component of the Stv1p sorting process was discovered by co-localizing Stv1p with endosomal marker proteins in a class “E” *vps* mutant background. In a class “E” *vps* mutant, proteins that normally traffic to the endosomal network do so normally but fail to exit, due to a specific block in endosomal retrograde and anterograde traffic. This phenotype of the class “E” mutants effectively turns the endosome into a sorting “black hole”; proteins that transit the endosome, even briefly, become trapped in an abnormally large endosome termed the class “E” compartment. In wild type cells Stv1p localizes to the late Golgi but in class “E” mutants its localization is shifted to the class “E” compartment, indicating that the endosome is part of Stv1p’s normal sorting itinerary. Since Stv1p does not co-localize with endosomal markers in wild-type cells at steady-state, it must only reside in the endosome for a relatively brief period of time before being returned to the late Golgi via retrograde transport. This type of Golgi-endosome sorting “loop” has been shown to direct the correct localization of other late Golgi proteins, such as Ste13p and Vps10p (BRYANT and STEVENS 1997; COOPER and STEVENS 1996). The signals in Ste13p and Vps10p that direct their retrieval from the endosome to the Golgi have been well characterized, and both signals contain aromatic residues critical for their function.

Additionally, Ste13p has been shown to contain a second sorting signal, one that delays exit of the protein from the late Golgi (BRYANT and STEVENS 1997). As stated above it appears certain that Stv1p is retained to the Golgi by retrograde-mediated retrieval from the endosome, but a Golgi-retention signal similar to that characterized for Ste13p may also play a role. My finding that aromatic residues are the most crucial for Stv1p Golgi localization supports the notion that I have identified a signal directing endosome to Golgi retrograde transport.

In order to isolate mutant alleles of Stv1p that failed to localize Stv1p V-ATPase to the Golgi I performed a forward genetic screen using cellular zinc resistance as a readout for V-ATPase localization. Cellular zinc resistance requires vacuolar acidification. Therefore, mutant alleles of Stv1p that are defective for Golgi-retention (i.e. vacuolar localized) must also retain near wild type levels of V-ATPase assembly and enzymatic function. The region of *STV1* corresponding to the N-terminal 455 amino acids was mutagenized, as this region was shown to contain the Golgi-retention signal (KAWASAKI-NISHI *et al.* 2001). The initial screen was performed with the mutant *STV1* gene on a low-copy (CEN) based plasmid containing the native *STV1* promoter and terminator sequences. The mutant *STV1* was the only cellular source of “a” subunit. This experimental design resulted in some complications; when plasmids were rescued from mutant cells and retransformed into an isogenic strain the plasmid did not always yield a zinc resistance phenotype. Additionally, I noticed fluctuations in individual colony size when testing the mutants for zinc resistance by serial dilution. I believe that these effects were due to plasmid copy-number fluctuations, because *vph1Δ stv1Δ*

containing plasmid born *STVI* gains a selective growth advantage when Stv1p expression is increased. I avoided a severe selection for increased Stv1p expression by never maintaining cells following zinc exposure, but in my hands, increased expression of Stv1p results in a slight increase to fitness on non-selective media as well. This variability caused a multitude of problems during the nascent stages of the project and I ultimately decided to integrate the most zinc resistant alleles of *STVI* into the endogenous genomic locus. Genomic integration of *STVI* completely stabilized the zinc resistance phenotype but had the unexpected effect of significantly reducing the size of the mutant pool. However, I now had mutants that behaved reproducibly and clearly mislocalized Stv1p V-ATPase to the vacuole by a variety of assays. Each of these randomly isolated mutants, and the mutants I later created, have been fully sequenced twice and then individually integrated and tested for zinc resistance a minimum of four times. The phenotypes are completely stable and are due solely to the individual residue changes found in each mutant.

Sequence analysis of the randomly isolated mutants was used to identify regions of the Stv1p peptide that might be required for Stv1p V-ATPase Golgi retention. Dozens of regions tested, but only when Tyr₈₅-Ile-Leu-His and Phe₅₀ were changed to alanine were the resulting mutants significantly zinc resistant. Further analysis defined Trp₈₃ and Tyr₈₅ as the residues most critical for Stv1p Golgi retention. These results are almost completely consistent with the primary sequence data, as 11 of 13 of the most zinc resistant mutants have residue changes in these areas. Of the two outliers, one contains a leucine to proline at position 43 and may affect Phe₅₀, and the second contains an alanine

to proline substitution at position 79, which would almost certainly affect the conformation of the Trp₈₃-Lys-Tyr region. The most phenotypically severe mutant I created was Phe₅₀ Ala₈₃-Lys-Ala, although this mutant appears to mislocalize only slightly more Stv1p than Ala₈₃-Lys-Ala alone. Trp₈₃-Lys-Tyr lies in a Stv1p-specific region not found in Vph1p by sequence alignment, making it a good candidate for the region of Stv1p that binds directly to the endosomal sorting machinery. Because of this, I choose to focus my efforts on this region and performed an alanine scan to define the relative contribution of its constituent amino acids to Stv1p Golgi retention. I also defined the flanks of this important region where amino acid substitutions no longer affected Stv1p localization.

As described above, aromatic amino acids in small regions of three to five residues frequently mediate binding of cargo proteins to the endosomal sorting machinery, such as the retromer complex. My discovery that the tryptophan and tyrosine residues in the Trp₈₃-Lys-Tyr motif of Stv1p are required for its Golgi retention indicates that Stv1p may bind to the endosomal sorting machinery in a canonical fashion. Phe₅₀ also plays a role in Stv1p sorting, albeit a significantly smaller one than Trp₈₃-Lys-Tyr. Unlike Trp₈₃-Lys-Tyr, Phe₅₀ is conserved between Stv1p and Vph1p, and is therefore unlikely to directly bind to sorting machinery. Secondary structure prediction algorithms indicate that an alpha helix may lie between Phe₅₀ and Trp₈₃-Lys-Tyr, and that the substitution Phe₅₀ -> Ala₅₀ would act as a “helix-breaker”. If these predictions are correct Ala₅₀ may affect the Golgi localization of Stv1p via an indirect perturbation to the Trp₈₃-Lys-Tyr motif. However, the fact that the Ala₅₀, Ala₈₃-Lys-Ala double mutant is slightly

more zinc-resistant than Ala₈₃-Lys-Ala alone indicates that Trp₈₃ and Tyr₈₅ is unlikely to be the only point of contact with the Golgi-retention machinery, and that Phe₅₀ may play a direct role along with Trp₈₃-Lys-Tyr in binding to a single sorting complex. An intriguing possibility is that Phe₅₀ may mediate a second sorting process, such as delaying V-ATPase exit from the Golgi in a mechanism similar to that described for Ste13p (BRYANT and STEVENS 1997).

Having demonstrated the necessity of the Trp₈₃-Lys-Tyr residues for Stv1p Golgi retention, I wished to address whether these residues were sufficient to cause Vph1p's retention to the Golgi. The Trp₈₃-Lys-Tyr residues lie in a Stv1p-specific insertion, and I was hopeful that if this region was introduced into Vph1p it would cause the chimeric protein to localize to the Golgi. I created a total of six Stv1p/Vph1 chimeras, and all were placed under the expression of the low-level *STV1* promoter to avoid overexpression. Three of them were not assembly competent, and a fourth was minimally functional (data not shown). Two chimeras were functional, one contained the Stv1p-specific insertion, and the second contained the entire Phe₅₀ to Ala₈₃-Lys-Ala region. Neither of these chimeras displayed Golgi localization, residing instead on the vacuolar membrane. There are many possible reasons why the residues I defined as necessary are not sufficient to cause Vph1p's retention to the Golgi. Judging from low resolution cryo-electron microscopy data, the N-terminus of the "a" subunit appears to physically interact with at least four V-ATPase subunits (H, E, G and d) (ZHANG *et al.* 2008). In addition, the N-terminus of "a" is predicted to self-interact, making the Trp₈₃-Lys-Tyr region proximal to a region of the Stv1p at approximately residue 350. If Stv1p

interacts with itself in that region, it may be that this self interaction is required for proper presentation of the sorting motif. My data clearly highlights the complexity of the Stv1p Golgi-retention signal, and I believe that future studies and higher resolution structural information will ultimately determine whether Trp₈₃-Lys-Tyr directly binds to endosomal sorting factors.

APPENDIX

MATERIALS AND METHODS

Strains-Strains were propagated and transformations were done as in Burke et. al 2000 (BURKE *et al.* 2000).

Gene knockouts-Genomic deletions were obtained by PCR amplification of the NAT or KAN cassette (GOLDSTEIN and MCCUSKER 1999) with PCR primers containing additional sequence that was homologous to the desired integration site. These linear DNA fragments were transformed into cells, and drug-resistant integrants were selected on solid media. Drug-resistant isolates were assayed for correct integration of the drug cassette by diagnostic PCR.

STVI random mutant construction-A CEN-based vector (pRS316) containing the full-length *STVI* (3xHA at AA position 227) and 500 bp of *STVI* 5' UTR and 135 bp of 3' UTR was constructed and then modified by Quick-change PCR to include two unique restriction sites: *NheI* 74 bp 5' to the *STVI* start codon, *SnaBI* (silent) 1,403 bp 3' to the *STVI* codon. The *STVI* plasmid was then linearized with the *NheI* and *SnaBI* restriction endonucleases, and co-transformed into *vph1Δ stv1Δ* yeast with a randomly mutagenized (Genemorph II; Stratagene) fragment of *STVI* containing 40 bp overlaps. The plasmid was re-circularized in yeast and the resulting mutants screened for zinc resistance. To integrate the mutants into the genome the same *NheI/SnaBI* was cloned by *in vitro* ligation into a second vector that lacked the ability to replicate in yeast (pRS306). The

pRS306 recipient vector contained a 3' 642 bp truncation of the *STVI* ORF and also contained a unique *MluI* restriction site (silent) at basepair 1,836. Once the mutagenized fragment had been transferred to the pRS306 “suicide vector” it was linearized by digest with *MluI* and transformed into *vph1Δ::NAT stv1-NTΔ::KAN* cells. Correct “loop-in” integration restored a functional copy of *STVI* making the cells both Ura⁺ and calcium resistant.

STVI random mutant screening-*vph1Δ stv1Δ* cells containing plasmid-borne mutant *STVI* were screened by replica plating onto YEPD media containing 5 mM ZnCl₂. The plasmid-borne mutants were then screened by printing at 16-fold degeneracy using a RoToR HDA robot (Singer Instruments) onto YEPD + 4 mM ZnCl₂. The levels of zinc were high relative to the concentration used for spot testing of the integrants because of plasmid-mediated increases in Stv1p expression. I also observed that high cell densities displayed a reduced zinc sensitivity.

STVI mutant construction-Mutations were introduced *de novo* into *STVI* by Quick-change PCR mutagenesis directly into the pRS306 suicide vector. Resulting mutations were confirmed by sequencing, and integrated as described for the randomly isolated mutants.

STVI/VPHI chimera construction-The *VPHI* coding sequence was PCR amplified with tailed primers and *in vivo* ligation between homologous sequences in that

linear fragment and a linearized *STVI* plasmid produced a CEN based plasmid with *STVI* 5' and 3' UTR flanking the *VPHI* ORF. A 3xHA tag/alcohol dehydrogenase terminator/NAT drug resistance cassette was then added 3' to the *VPHI* stop codon by *in vivo* ligation. A unique restriction site was added to the *VPHI* ORF at the region where L1/R1 from *STVI* was to be appended and L1/R1 and other *STVI* fragments were introduced by *in vivo* homologous recombination between this linearized plasmid and a *STVI* PCR fragment (L1/R1, L2/R1, etc.) containing primer tails that served to target the recombination events.

Culture conditions -Yeast were cultured in YEPD (1% yeast extract, 2% peptone, and 2% dextrose), YEPD buffered to pH 5.0 using 50 mM succinate/phosphate. Growth tests were performed by culturing exponentially growing yeast in rich medium to a cell density of 1.0 OD₆₀₀, serially diluted fivefold, and spotted onto agar plates. Plates used included YEPD pH 5.0, or YEPD plus the indicated amount of ZnCl₂.

Whole cell extract preparation and immunoblotting-Whole cell extracts were prepared as previously described (RYAN *et al.* 2008). Briefly, cultures were grown overnight in SD dropout media and then diluted to 0.25 OD₆₀₀/ml in YEPD pH 5.0 and grown to a cell density of OD₆₀₀ = 1.0. A total of 10 OD₆₀₀ of the culture was centrifuged, resuspended in 0.25 ml Thorner buffer (8 m urea, 5% SDS, and 50 mM TRIS pH 6.8), and vortexed with 0.2 ml of glass beads. Following centrifugation, protein concentrations were determined using a modified Lowry protein assay (MARKWELL *et al.* 1978). Equal amounts of protein

were separated by SDS–PAGE, transferred to nitrocellulose membrane, and probed with antibodies. Antibodies used included monoclonal primary anti-HA (12CA.5.16.4; Invitrogen), anti-Dpm1p (5C5; Invitrogen), and secondary horseradish peroxidase-conjugated antimouse antibody (Jackson ImmunoResearch Laboratories, West Grove, PA). Blots were visualized by ECL detection.

Quinacrine microscopy-Yeast were stained with quinacrine as previously described (FLANNERY *et al.* 2004). Briefly, cells were grown overnight in YEPD pH 5.0 plus adenine, and diluted to a cell density of 0.25 OD₆₀₀/ml in YEPD. Yeast were harvested at a density of 0.8–1.0 OD₆₀₀/ml and 1ml of culture was placed on ice for 5 min. Cells were pelleted and resuspended in 200 mM quinacrine, 100 mM HEPES pH 7.6, and 50 mg/ml of concanavalin A tetramethylrhodamine (Invitrogen) in YEPD for 10 min at 30°. Following staining with quinacrine, cells were placed on ice and washed three times in 100 mM HEPES pH 7.6 plus 2% glucose (4°). Microscopy images were obtained using an Axioplan 2 fluorescence microscope (Carl Zeiss, Thornwood, NY). A 3100 objective was used as well as AxioVision software (Carl Zeiss).

Immunofluorescence microscopy-Yeast were fixed and stained as previously described (KAWASAKI-NISHI *et al.* 2001) with the following modifications: The primary antibody was changed to a mouse monoclonal α -HA.11 (16B12; Covance) diluted 1:250 and incubated with fixed cells overnight at 4°. The secondary antibody was goat α -mouse conjugated to Alexa-488 (Invitrogen) used at a 1:500 dilution. Microscopy images were

obtained using an Axioplan 2 fluorescence microscope (Carl Zeiss, Thornwood, NY). A 3100 objective was used as well as AxioVision software (Carl Zeiss).

Table 1-Summary of randomly isolated mutant amino acid changes and zinc resistance

<u>Mutant #</u>	<u>Growth</u>	<u>Amino Acid Changes</u>
9	+++	Q98H, K299R, K310N, H351R, K362N, Q379K
25	++	E127V, A168T, L314Q, H344Y, H351Q
31	++	A49G, L87S, R246K, N268Y, V312F
57	+	L43P, K121R
79	++	N72I, N117S, I329M, N415D
89	+++	D205V, D401Y, N415D
95	+	A49V, K362N, Q379R, I393V
99	++	I86N, D212G
101	+++	H88L, I193S, Q209H, V303A, D337Y, I417N
104/249	++	L47S, D146Y, Q379R
132	+++	E76V, A79P, N164D, E340D, Q341K, H344Y, I403V
146	++	I86F
155	+++	F50L, Q152L, F203L, L259S, E409D
172	++	R59G, L218I, N415D
176	+++	T124S, T219A, I417N
187	+++	A49T, R60S, W83R, Q132H, V163I, H236N, L296M, T338A
200	++	N117S, Q152L, L276M, F414S
213	+	N56T, P110H, I176V, L307I, N372D, N415D
254	++	L47S, D146Y, Q379R
270	++	H88L, Q150L, W257L, I304L, T324A
301	+++	D46E, F50L, S198R, D217V, Y238F, K298E, T345A, T405M

REFERENCES CITED

- BRYANT, N. J., and T. H. STEVENS, 1997 Two separate signals act independently to localize a yeast late Golgi membrane protein through a combination of retrieval and retention. *J Cell Biol* **136**: 287-297.
- BURKE, D., D.D. and T. STEARNS, 2000 *Methods in Yeast Genetics*.
- COOPER, A. A., and T. H. STEVENS, 1996 Vps10p cycles between the late-Golgi and prevacuolar compartments in its function as the sorting receptor for multiple yeast vacuolar hydrolases. *J Cell Biol* **133**: 529-541.
- CRUCIAT, C. M., B. OHKAWARA, S. P. ACEBRON, E. KARAUANOV, C. REINHARD *et al.*, 2010 Requirement of prorenin receptor and vacuolar H⁺-ATPase-mediated acidification for Wnt signaling. *Science* **327**: 459-463.
- DAVIS-KAPLAN, S. R., M. A. COMPTON, A. R. FLANNERY, D. M. WARD, J. KAPLAN *et al.*, 2006 PKR1 encodes an assembly factor for the yeast V-type ATPase. *J Biol Chem* **281**: 32025-32035.
- DI GIOVANNI, J., S. BOUDKAZI, S. MOCHIDA, A. BIALOWAS, N. SAMARI *et al.*, 2010 V-ATPase membrane sector associates with synaptobrevin to modulate neurotransmitter release. *Neuron* **67**: 268-279.
- FLANNERY, A. R., L. A. GRAHAM and T. H. STEVENS, 2004 Topological characterization of the c, c', and c'' subunits of the vacuolar ATPase from the yeast *Saccharomyces cerevisiae*. *J Biol Chem* **279**: 39856-39862.
- GOLDSTEIN, A. L., and J. H. MCCUSKER, 1999 Three new dominant drug resistance cassettes for gene disruption in *Saccharomyces cerevisiae*. *Yeast* **15**: 1541-1553.
- GRAHAM, L. A., and T. H. STEVENS, 1999 Assembly of the yeast vacuolar proton-translocating ATPase. *J Bioenerg Biomembr* **31**: 39-47.
- HILL, K. J., and T. H. STEVENS, 1994 Vma21p is a yeast membrane protein retained in the endoplasmic reticulum by a di-lysine motif and is required for the assembly of the vacuolar H⁽⁺⁾-ATPase complex. *Mol Biol Cell* **5**: 1039-1050.
- HINTON, A., S. R. SENNOUNE, S. BOND, M. FANG, M. REUVENI *et al.*, 2009 Function of a subunit isoforms of the V-ATPase in pH homeostasis and in vitro invasion of MDA-MB231 human breast cancer cells. *J Biol Chem* **284**: 16400-16408.

- KANE, P. M., 1995 Disassembly and reassembly of the yeast vacuolar H(+)-ATPase in vivo. *J Biol Chem* **270**: 17025-17032.
- KAWASAKI-NISHI, S., K. BOWERS, T. NISHI, M. FORGAC and T. H. STEVENS, 2001 The amino-terminal domain of the vacuolar proton-translocating ATPase a subunit controls targeting and in vivo dissociation, and the carboxyl-terminal domain affects coupling of proton transport and ATP hydrolysis. *J Biol Chem* **276**: 47411-47420.
- KORNAK, U., A. SCHULZ, W. FRIEDRICH, S. UHLHAAS, B. KREMENS *et al.*, 2000 Mutations in the a3 subunit of the vacuolar H(+)-ATPase cause infantile malignant osteopetrosis. *Hum Mol Genet* **9**: 2059-2063.
- LENG, X. H., M. F. MANOLSON and M. FORGAC, 1998 Function of the COOH-terminal domain of Vph1p in activity and assembly of the yeast V-ATPase. *J Biol Chem* **273**: 6717-6723.
- MALKUS, P., L. A. GRAHAM, T. H. STEVENS and R. SCHEKMAN, 2004 Role of Vma21p in assembly and transport of the yeast vacuolar ATPase. *Mol Biol Cell* **15**: 5075-5091.
- MANOLSON, M. F., D. PROTEAU, R. A. PRESTON, A. STENBIT, B. T. ROBERTS *et al.*, 1992 The VPH1 gene encodes a 95-kDa integral membrane polypeptide required for in vivo assembly and activity of the yeast vacuolar H(+)-ATPase. *J Biol Chem* **267**: 14294-14303.
- MANOLSON, M. F., B. WU, D. PROTEAU, B. E. TAILLON, B. T. ROBERTS *et al.*, 1994 STV1 gene encodes functional homologue of 95-kDa yeast vacuolar H(+)-ATPase subunit Vph1p. *J Biol Chem* **269**: 14064-14074.
- MARKWELL, M. A., S. M. HAAS, L. L. BIEBER and N. E. TOLBERT, 1978 A modification of the Lowry procedure to simplify protein determination in membrane and lipoprotein samples. *Anal Biochem* **87**: 206-210.
- NELSON, H., and N. NELSON, 1990 Disruption of genes encoding subunits of yeast vacuolar H(+)-ATPase causes conditional lethality. *Proc Natl Acad Sci U S A* **87**: 3503-3507.
- NICCHITTA, C. V., 2002 A platform for compartmentalized protein synthesis: protein translation and translocation in the ER. *Curr Opin Cell Biol* **14**: 412-416.
- NISHI, T., and M. FORGAC, 2000 Molecular cloning and expression of three isoforms of the 100-kDa a subunit of the mouse vacuolar proton-translocating ATPase. *J Biol Chem* **275**: 6824-6830.

- NISHI, T., and M. FORGAC, 2002 The vacuolar (H⁺)-ATPases--nature's most versatile proton pumps. *Nat Rev Mol Cell Biol* **3**: 94-103.
- NOTHWEHR, S. F., C. J. ROBERTS and T. H. STEVENS, 1993 Membrane protein retention in the yeast Golgi apparatus: dipeptidyl aminopeptidase A is retained by a cytoplasmic signal containing aromatic residues. *J Cell Biol* **121**: 1197-1209.
- OCHOTNY, N., A. VAN VLIET, N. CHAN, Y. YAO, M. MOREL *et al.*, 2006 Effects of human a3 and a4 mutations that result in osteopetrosis and distal renal tubular acidosis on yeast V-ATPase expression and activity. *J Biol Chem* **281**: 26102-26111.
- OKA, T., Y. MURATA, M. NAMBA, T. YOSHIMIZU, T. TOYOMURA *et al.*, 2001 a4, a unique kidney-specific isoform of mouse vacuolar H⁺-ATPase subunit a. *J Biol Chem* **276**: 40050-40054.
- PARRA, K. J., and P. M. KANE, 1998 Reversible association between the V1 and V0 domains of yeast vacuolar H⁺-ATPase is an unconventional glucose-induced effect. *Mol Cell Biol* **18**: 7064-7074.
- PERRET, E., A. LAKKARAJU, S. DEBORDE, R. SCHREINER and E. RODRIGUEZ-BOULAN, 2005 Evolving endosomes: how many varieties and why? *Curr Opin Cell Biol* **17**: 423-434.
- PRESTON, R. A., R. F. MURPHY and E. W. JONES, 1989 Assay of vacuolar pH in yeast and identification of acidification-defective mutants. *Proc Natl Acad Sci U S A* **86**: 7027-7031.
- ROBERTS, C. J., S. F. NOTHWEHR and T. H. STEVENS, 1992 Membrane protein sorting in the yeast secretory pathway: evidence that the vacuole may be the default compartment. *J Cell Biol* **119**: 69-83.
- ROJAS, J. D., S. R. SENNOUNE, D. MAITI, K. BAKUNTS, M. REUVENI *et al.*, 2006 Vacuolar-type H⁺-ATPases at the plasma membrane regulate pH and cell migration in microvascular endothelial cells. *Am J Physiol Heart Circ Physiol* **291**: H1147-1157.
- RYAN, M., L. A. GRAHAM and T. H. STEVENS, 2008 Voa1p functions in V-ATPase assembly in the yeast endoplasmic reticulum. *Mol Biol Cell* **19**: 5131-5142.
- SMITH, A. N., J. SKAUG, K. A. CHOATE, A. NAYIR, A. BAKKALOGLU *et al.*, 2000 Mutations in ATP6N1B, encoding a new kidney vacuolar proton pump 116-kD subunit, cause recessive distal renal tubular acidosis with preserved hearing. *Nat Genet* **26**: 71-75.

- SOBACCHI, C., A. FRATTINI, P. ORCHARD, O. PORRAS, I. TEZCAN *et al.*, 2001 The mutational spectrum of human malignant autosomal recessive osteopetrosis. *Hum Mol Genet* **10**: 1767-1773.
- SUN-WADA, G. H., T. TOYOMURA, Y. MURATA, A. YAMAMOTO, M. FUTAI *et al.*, 2006 The $\alpha 3$ isoform of V-ATPase regulates insulin secretion from pancreatic beta-cells. *J Cell Sci* **119**: 4531-4540.
- SUN-WADA, G. H., Y. WADA and M. FUTAI, 2003 Vacuolar H⁺ pumping ATPases in luminal acidic organelles and extracellular compartments: common rotational mechanism and diverse physiological roles. *J Bioenerg Biomembr* **35**: 347-358.
- TOEI, M., R. SAUM and M. FORGAC, 2010 Regulation and isoform function of the V-ATPases. *Biochemistry* **49**: 4715-4723.
- WANG, Y., D. J. CIPRIANO and M. FORGAC, 2007 Arrangement of subunits in the proteolipid ring of the V-ATPase. *J Biol Chem* **282**: 34058-34065.
- WILCOX, C. A., K. REDDING, R. WRIGHT and R. S. FULLER, 1992 Mutation of a tyrosine localization signal in the cytosolic tail of yeast Kex2 protease disrupts Golgi retention and results in default transport to the vacuole. *Mol Biol Cell* **3**: 1353-1371.
- ZHANG, Z., Y. ZHENG, H. MAZON, E. MILGROM, N. KITAGAWA *et al.*, 2008 Structure of the yeast vacuolar ATPase. *J Biol Chem* **283**: 35983-35995.